Picosecond Infrared Study of the Photodynamics of Carbonmonoxy-Cytochrome *c* Oxidase†

R. Brian Dyer,*,‡ Kristen A. Peterson‡,§ Page O. Stoutland,‡ and William H. Woodruff‖

Chemical Sciences and Technology Division (CST), Los Alamos National Laboratory, Los Alamos, New Mexico 87545

Received June 23, 1993; Revised Manuscript Received September 16, 1993®

ABSTRACT: Time-resolved infrared (TRIR) techniques have been employed to study the reactions of carbon monoxide with the cytochrome a_3–Cu_B site of cytochrome *c* oxidase (CcO). The ligation dynamics immediately following photodissociation have been investigated using picosecond TRIR spectroscopy and linear dichroism. The rate of photoinitiated transfer of CO from cytochrome a_3 to Cu_B was measured directly by monitoring the development of the transient Cu_BCO absorption. In less than 1 ps, a stationary Cu_BCO spectrum develops, which together with the CO infrared linear dichroism is constant until the CO dissociates from Cu_B on a microsecond time scale. These observations indicate that the CO is transferred between metals and reaches its equilibrium conformation in less than 1 ps. This unprecedented ligand transfer rate has profound implications with regard to the structure and dynamics of the cytochrome a_3–Cu_B site, the functional architecture of the protein, and coordination dynamics in general.

Cytochrome oxidase (CcO[1] or ferrocytochrome *c*: dioxygen oxidoreductase, EC 1.9.3.1) is the terminal oxidase of cellular respiration in all plants and animals and numerous lower organisms (Wikström et al., 1981; Woodruff et al., 1993). It catalyzes the four-electron reduction of O_2 by cytochrome *c* and conserves the energy of this reaction as a transmembrane proton gradient. Many aspects of the molecular mechanisms of these functions are unknown; it is clear, however, that the coordination chemistry and ligation dynamics of the ligand binding site, the binuclear cytochrome a_3–Cu_B center, are crucial elements of the function of the enzyme in activating O_2 and in effecting its reduction to water. It has also been suggested (Woodruff et al., 1991) that the ligation reactions of the binuclear site may be components of the proton pumping mechanism by which the enzyme transduces the energy of the redox reaction.

Significant advances have been made recently in defining the structure and reactivity of the binuclear site. Studies of bacterial oxidases that are simpler in structure but functionally homologous to the mitochondrial enzymes have yielded important structural insights (Shapleigh et al., 1992; Surerus et al., 1992). Gennis and co-workers have assigned four histidine imidazoles as ligands of cytochrome a_3 and Cu_B through site-directed mutagenesis of each of the conserved histidine residues in the aa_3-type cytochrome oxidase of *Rhodobacter sphaeroides* and in the related *bo*-type oxidase from *Escherichia coli* (Shapleigh et al., 1992). In addition, a non-histidine ligand to Cu_B has been implicated in time-resolved spectroscopic studies of CO photodissociation (Woodruff et al., 1991). These structural insights provide a backdrop for understanding the reactivity of the binuclear site.

Photodissociation studies of CO have played a major role in elucidating the ligand binding reactions of the binuclear center. Flow-flash experiments based on CO photodissociation, pioneered by Gibson (Gibson & Greenwood, 1963; Greenwood & Gibson, 1967), have established much of what is known regarding the intermediates in the binding and reduction of O_2 (Blackmore et al., 1991; Varotsis et al., 1989). The CO reactions themselves exemplify the mechanisms open to O_2 and other small-molecule ligands, providing important information about the pathways available for exogenous ligands to and from the active site. Time-resolved magnetic circular dichroism (MCD) and resonance Raman have been used to investigate dynamics after CO dissociation from fully reduced CcO on nanosecond and longer time scales (Woodruff et al., 1991), while UV–vis absorption experiments have been performed on all relevant time scales from femtoseconds to milliseconds (Einarsdóttir et al., 1993; Stoutland et al., 1991). These experiments probe only the heme sites directly, because the reduced Cu_B center and the protein itself are generally silent to the spectroscopies employed. Electronic absorption and resonance Raman studies on CcO are further complicated by contributions from both cytochromes *a* and a_3, which can be difficult to distinguish. In contrast, infrared spectroscopy is uniquely suited as a probe for the reactions of CO with CcO, particularly the ligation reactions of Cu_B. The high oscillator strength of the CO infrared absorption combined with the exceptional sensitivity of its frequency and bandwidth to changes in bonding and environment make it an ideal probe of ligation reactions. Furthermore, infrared linear dichroism experiments can provide specific structural details through the measurement of the angular orientation of the CO with respect to the heme plane.

We have followed the steps which CO takes on its path out of the protein by probing changes in the infrared spectrum and infrared linear dichroism following photoinduced dissociation from cytochrome a_3. FTIR studies have demonstrated that, below 180 K, photodissociated CO binds to Cu_B both in

† This work was supported by NIH Grant GM 45807.

* Author to whom correspondence should be addressed.

‡ CST-4, MS J567.

§ Present address: Hansen Experimental Physics Lab, Stanford University, Stanford, CA 94305-4085.

‖ CST-14, MS C345.

® Abstract published in *Advance ACS Abstracts,* December 15, 1993.

[1] Abbreviations: CcO, cytochrome *c* oxidase; TRIR, time-resolved infrared; FTIR, Fourier-transform infrared; IR, infrared; Nd:YAG, neodymium:yttrium aluminum garnet; MCT, mercury cadmium telluride; FWHM, full-width at half-maximum.

0006-2960/94/0433-500$04.50/0

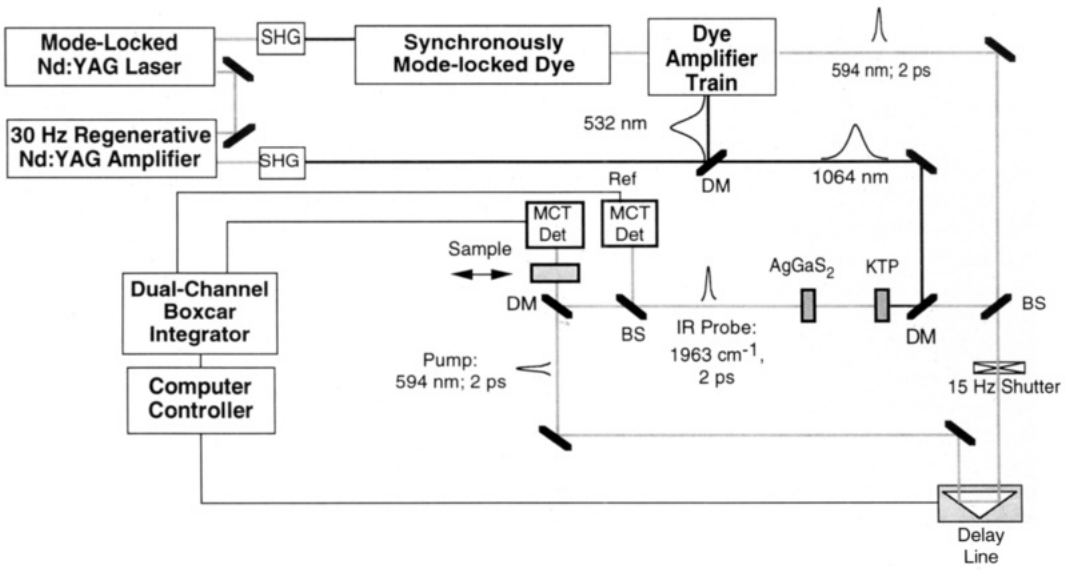

FIGURE 1: Schematic of the picosecond time-resolved infrared apparatus (BS = beam splitter; DM = dichroic mirror; MCT = mercury cadmium telluride; SHG = second harmonic generator).

mitochondrial preparations (Alben et al., 1981) and in the detergent-solubilized enzyme (Einarsdóttir et al., 1989). We have also observed Cu_BCO in the *room temperature* FTIR of cytochrome ba_3 from *Thermus thermophilus* (Einarsdóttir et al., 1989). In a recent time-resolved infrared (TRIR) study of the eukaryotic enzyme at ambient temperature, we obtained conclusive evidence for the quantitative transfer of photodissociated CO to Cu_B (Dyer et al., 1989a). A transient infrared absorbance due to the C–O stretching vibration of Cu_BCO was observed to appear within the 200-ns time resolution of our instrument and decay on a microsecond time scale. In a parallel kinetics study, our results conclusively demonstrate that, in addition to its established redox function, Cu_B acts as a gateway to the a_3 heme site; coordination to Cu_B is an obligatory mechanistic step for CO (and, by inference, other small molecule ligands including O_2) both entering the a_3 heme site and departing the protein after photodissociation (Einarsdóttir et al., 1993; Woodruff et al., 1991).

This study focuses on the earliest "ultrafast" steps following photodissociation of CO from cytochrome a_3 of CcO. Ultrafast events have been shown to be key steps in important biological processes for which the overall rates are slow. Examples are the initial charge separation in photosynthetic reaction centers (3 ps) (Breton et al., 1988), the isomerization of the retinal chromophore in bacteriorhodopsin (200 fs) (Schoenlein et al., 1991), and heme conformational changes in the cooperative binding of O_2 to hemoglobin (<1 ps) (Petrich & Martin, 1989). Proteins may use ultrafast reaction dynamics to optimize function. Although the overall rate of O_2 turnover by CcO is moderate ($\sim 600\ s^{-1}$), we have observed ultrafast dynamics in a crucial component of this process, the ligation dynamics of small molecules with the binuclear site. Initial results on the photoinitiated ligand transfer of CO from cytochrome a_3 to Cu_B indicate that it is the fastest ligation reaction yet observed (Dyer et al., 1991). The rise time of the appearance of Cu_BCO appears to be less than 1 ps. Here we explore the dynamics of the CO photodissociation and transfer more fully, including the picosecond TRIR spectrum and TRIR linear dichroism. The ultrafast nature of this reaction has profound implications regarding the structure and dynamics of the binuclear site, hence the functional architecture of the protein. The observation of ultrafast bond formation also has important consequences for coordination dynamics in general. Cytochrome oxidase may provide a unique environment in which the mechanisms of ligand transfer and bond formation can be studied directly, in the absence of diffusion effects.

EXPERIMENTAL PROCEDURES

Beef heart cytochrome oxidase was isolated according to the procedure of Einarsdóttir et al. (1993), which is a modification of that of Yoshikawa et al. (1977). The IR sample solution was 1.0 mM cytochrome oxidase, 10 mM sodium phosphate, pH 7.4, and 0.1% lauryl maltoside. The deoxygenated enzyme solution was reduced by a small excess of dithionite and then incubated under 1 atm CO to yield the fully reduced CO-bound complex, which was transferred anaerobically to a 200-μm pathlength IR cell fitted with CaF_2 windows. Static visible absorption spectra were taken periodically during the life of the sample to ensure sample quality and integrity.

Ultrafast TRIR experiments were based on the standard pump-probe technique which we have previously described (Stoutland et al., 1992), in which time resolution is obtained by optically delaying (0.3 mm = 1 ps) an infrared probe pulse with respect to a visible pump pulse. We have modified our TRIR apparatus as shown in Figure 1. The pump (excitation) pulse is obtained by amplifying the output of a dual-jet dye laser (R6G/DODCI) synchronously pumped by a frequency-doubled cw mode-locked Nd:YAG laser (Coherent Antares 76S). Amplification is effected in a three-stage Kiton Red dye amplifier, with a Schott filter acting as a saturable absorber between stages 1 and 2. The amplifier is longitudinally pumped by a frequency-doubled Nd:YAG regenerative amplifier (Continuum RA30, 20 mJ at 532 nm, 60-ps pulses at 30 Hz), seeded by the cw-mode locked Nd:YAG laser. Stages 1 and 2 receive approximately 1 mJ/pulse, and stage 3 receives 10 mJ/pulse of 532-nm pump energy, resulting in ca. 2-ps pulses of up to 0.5 mJ/pulse at a 30-Hz repetition rate.

The infrared probe pulse is generated in a two step nonlinear mixing process. In the first step, the difference frequency between the 1064 nm (1 mJ) pulses from the regenerative amplifier and the amplified dye pulse (ca. 10%) is generated in a potassium titanyl phosphate (KTP) crystal (3 mm thick) cut at 65° relative to the optic axis for type II phase matching. This generates a near-infrared pulse at approximately 1.3 μm. The mid-infrared probe pulse (1.7 ps, FWHM $\sim 8\ cm^{-1}$, 100 nJ) is generated in a second step by differencing the

residual 1064-nm pulse with the 1.3-μm pulse in a silver thiogallate ($AgGaS_2$) crystal (3 mm thick) cut at 46° for type II phase matching. The infrared frequency is changed by tuning the dye laser with a two-plate birefringent filter so as to change the difference frequency. With the present dye combinations and mixing crystals, the infrared probe pulse is tunable from 1300 to 3000 cm^{-1}, which corresponds to tuning the dye laser from 572 to 633 nm.

Noise in absorption measurements made with this system arises primarily from shot to shot amplitude fluctuations (10–15%) in the dye laser. This is minimized by using a normalization process in which the probe beam is split into two parts; a signal beam which passes through the sample and a reference beam which does not. The beams are detected by two matched 2-mm diameter MCT detectors (Infrared Associates). The nonlinearity of semiconductor detectors requires that the signal and reference intensities be carefully balanced so that they accurately track one another. The sample and reference signals are integrated in a dual-channel gated integrator (SRS 250), ratioed in an analog signal processor (SRS 235), and then digitized with 13-bit resolution. This normalization process reduces the shot to shot variation to 2–4%. The signal-to-noise is further improved by computer averaging of the ratioed signal.

Long-term drift is minimized by chopping the pump beam at one half of the laser repetition rate with a mechanical shutter, and subsequently ratioing light-on to light-off data. Experiments were typically run in saturation (i.e., near 100% photodissociation) to minimize the effect of intensity fluctuations of the visible pump beam; control experiments demonstrated that this had no effect on the observed dynamics. The sample was translated perpendicularly to the beams to reduce sample damage and photoproduct build up.

Typical transients consist of scanning the delay line in 0.3-ps steps, taking 200 shots alternating pump light on/off at each step. Many (10–30) sequential scans are averaged to improve the signal to noise ratio, resulting in a detection limit of $\Delta A = 10^{-4}$ on top of background infrared absorbances of 1–2. The zero of time and the temporal response of the apparatus (determined solely by the pump-probe cross-correlation) are measured directly before and after each series of scans as follows. A silicon wafer is substituted for the sample; to match the dispersion of the sample, a CaF_2 window of the same thickness as the entrance window of the sample cell is attached to its face. The silicon is illuminated with the visible pump beam which causes an instantaneous and long-lived (about 200 ns for these conditions) decrease in infrared probe transmission (Yen et al., 1983). The temporal response measured in this way is typically well described by a $sech^2$ function with a FWHM of ca. 3.5 ps. When the instrument response is properly accounted for with convolution techniques, events with a lifetime or rise time of 1 ps or longer are easily resolved.

Induced linear dichroism measurements are made by rotating the pump polarization (better than 1000/1) parallel or perpendicular to the probe polarization (better than 200/1) with a half-wave plate. The pump power measured at the sample position is independent of beam polarization, showing that there is no polarization bias in the optics following the half-wave plate which could distort the results.

RESULTS

The photodissociation of CO was observed by tuning the infrared probe pulse to the ground state infrared absorbance of the cytochrome a_3–CO ($Fe_{a3}CO$) complex at 1963 cm^{-1}.

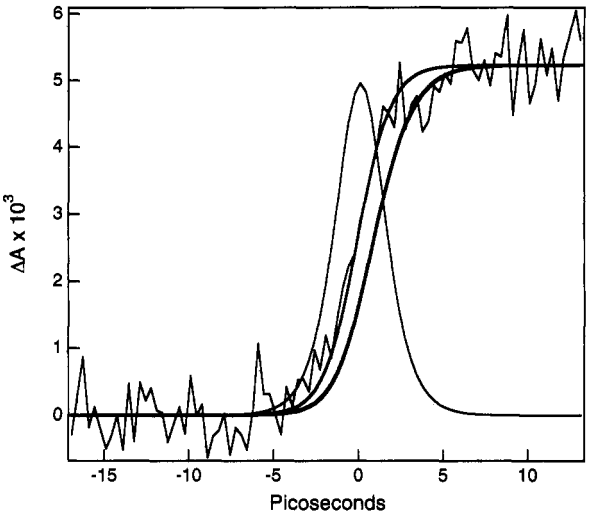

FIGURE 2: Time-resolved infrared absorbance monitored at the peak of Cu_BCO absorbance at 2062 cm^{-1}. The smooth traces are the experimentally determined instrument response function, and rightmost, the convolution of this function with a 1-ps exponential rise and 6-μs exponential decay.

Following excitation into the α-band at 594 nm, we observed an instrumentally limited rise of the bleach of the 1963-cm^{-1} band which was subsequently invariant for >250 ps. Longer time scale TRIR measurements show that this bleach persists for milliseconds (Dyer et al., 1989a). The absence of any detectable (<1%) recovery of the bleach from 1 ps until CO begins to recombine on the millisecond time scale indicates that there is no fast geminate recombination. The dissociation time scale is consistent with femtosecond visible absorption experiments which have shown that photodissociation of CO from hemes is very rapid and efficient, occurring within 100 fs for cytochrome oxidase (Stoutland et al., 1991), hemoglobin, and myoglobin (Petrich & Martin, 1989), with a quantum yield near unity. The absence of *any* geminate recombination, however, is unique to cytochrome oxidase, a consequence of the ligation mechanism of the binuclear center.

The appearance of the Cu_BCO complex was monitored by tuning the probe pulse to 2062 cm^{-1}, the Cu_BCO stretching frequency. Surprisingly, the rise time of this transient absorption was also indistinguishable from our instrument response. Figure 2 shows the change in absorption at 2062 cm^{-1} along with the instrument response and a convolution of the instrument response with a 1 ps exponential rise. An accurate determination of the zero of time is critical to this analysis; therefore, it was carefully measured before and after each CcO transient without changing any experimental parameter. The instrument response convolved with a 1 ps risetime is clearly slower than the observed rate, allowing us to conclude that the Cu_BCO complex is formed in less than 1 ps. The rise time was independent of the pump-pulse power.

The static extinction coefficient of the Cu_BCO absorption is 640 M^{-1} cm^{-1}, a factor of 7 less than for $Fe_{a3}CO$ (Dyer et al., 1989a). The ratio of the observed changes in absorption in our experiments is equal to this ratio when care is taken to perform the two measurements (i.e., at 1963 and 2062 cm^{-1}) under the same conditions of beam overlap, pump power, etc. This is consistent with CO being quantitatively transferred from the iron to the copper center.

Further evidence for this interpretation is found by comparing the 5-ps TRIR spectrum with the 200-ns TRIR spectrum (Figure 3). These spectra were generated in a point by point manner by obtaining transients at various probe

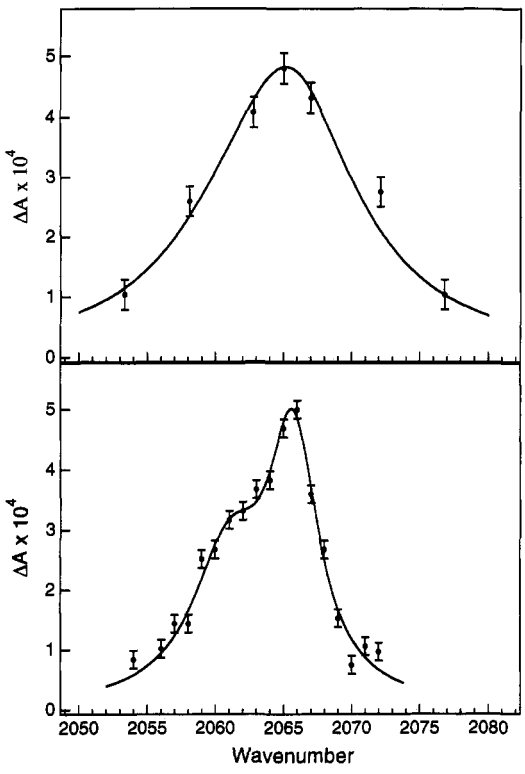

FIGURE 3: Time-resolved infrared spectra 5 ps (upper panel) and 200 ns (lower panel) after photodissociation of CO from cytochrome a_3. The curves are Lorentzian fits to the data (see text).

frequencies within the Cu_BCO absorption band. The picosecond transients were obtained with the instrument described above. In this case, the rise times of the individual transients were all instrument response limited. The ΔAs were computed from the individual transients by averaging the magnitude of the absorbance between 5 and 30 ps, after the ΔA has reached its full amplitude. If the data are analyzed at earlier times, such that the transient rise is incomplete, the spectrum obtained is identical except that the intensity is diminished. Each data point is an average of ΔAs obtained in this manner from three to five separate runs at a given wavelength. The error bars indicate two standard deviations of the values observed among runs. The nanosecond transients were obtained with a previously described apparatus which employs a Q-switched Nd:YAG pump laser (7 ns, 532 nm), a CW diode probe laser, and a fast rise time InSb detector (Dyer et al., 1989a). The transients in this case are also instrument response (200 ns) limited, and the ΔAs were computed by averaging the magnitude of the absorbance change from 200 to 300 ns.

These spectra were simulated (lines in Figure 3) using the sum of two Lorentzian line shapes corresponding to the two components of the Cu_BCO absorption seen in the high-resolution low-temperature FTIR spectra of the kinetically trapped Cu_BCO complex (Fiamingo et al., 1982). Two major peaks are observed at low temperatures, one near 2061 cm^{-1} and a less intense one near 2043 cm^{-1}, which have been assigned to discrete conformers of CcO. The frequency of the minor peak increases linearly with temperature in the range (10–180 K) observable in this experiment. If the data are extrapolated to room temperature, this minor component shifts to near 2059 cm^{-1} where it is expected to appear as an incompletely resolved shoulder. This is exactly what is observed in the room temperature transient spectra (Figure 3). The wavelengths of the individual Lorentzian components used to simulate each spectrum were approximated from extrapolation of the low-temperature FTIR values to room temperature, and then the intensities and bandwidths were varied to give the most reasonable fit to the data. The extapolation from Alben's low temperature data for CcO in a glycerol glass to room temperature solution may not seem reasonable; however, we have observed that the IR frequencies, line widths, and dichroism of CO bound to Fe or Cu are not affected by the solvent nor are they affected discontinuously by freezing, regardless of solvent composition for glycerol/water mixtures and pure water. The Fe_{a3}–Cu_B site is clearly isolated from external solvent influences and a discontinuous effect of the solvent glass transition on the Cu_B–CO frequency is therefore not expected. Most importantly, this approach yields reasonable fits of the transient IR spectra; the parameters that best reproduce the 5-ps and 200-ns spectra are (5-ps spectrum) $\nu_1 = 2060\ cm^{-1}$, $\Delta\nu_1 = 12\ cm^{-1}$, $\epsilon_m = 0.07\ mM^{-1}\ cm^{-1}$ and $\nu_2 = 2065\ cm^{-1}$, $\Delta\nu_2 = 12\ cm^{-1}$, $\epsilon_m = 0.23\ mM^{-1}\ cm^{-1}$; (200-ns spectrum) $\nu_1 = 2060\ cm^{-1}$, $\Delta\nu_1 = 6\ cm^{-1}$, $\epsilon_m = 0.09\ mM^{-1}\ cm^{-1}$ and $\nu_2 = 2065\ cm^{-1}$, $\Delta\nu_2 = 4.5\ cm^{-1}$, $\epsilon_m = 0.17\ mM^{-1}\ cm^{-1}$. Within experimental error, these parameters are the same, except that the peak widths are a factor of 2 greater in the case of the 5-ps spectrum. This broadening is an experimental artifact inherent to the picosecond TRIR experiment. The effective resolution for the 5-ps spectrum is 8 cm^{-1}, determined by the transform limited width of the probe pulse, compared to 4 cm^{-1} for the 200-ns spectrum, determined by the band-pass of the monochromater used to filter the multimode output of the IR diode probe laser. It is clear from these observations that the Cu_BCO spectrum is fully developed within the 1-ps time resolution of this experiment and persists for microseconds, until the CO dissociates. We conclude that the CO is quantitatively transferred and the equilibrium Cu_BCO conformation is obtained in 1 ps or less. Furthermore, no transient absorption to the red of the ground state peak was observed which could be assigned to vibrational excitation in the Cu_BCO mode. Significant transient population in $v = 1$ or 2 of the Cu_BCO stretch would be evidenced by a red-shift of the absorption band due the anharmonicity of CO vibrations, typically 15 cm^{-1} (Heilweil et al., 1987).

The average orientations of the CO infrared transition dipole when attached to Fe_{a3} and Cu_B relative to the visible absorption dipole which lies in the Fe_{a3} heme plane were determined by induced linear dichroism measurements. This approach has been applied previously to CO ligated heme proteins (Hansen et al., 1989; Ormos et al., 1988) and specifically to cytochrome oxidase (Dyer et al., 1989b). In the limit of no photodissociation, the polarization ratio, $R = \Delta A_\perp / \Delta A_\parallel$, associated with a photoselected subset of molecules, is related to the average angle, α, of the probed transition dipole relative to the normal to the excitation dipoles by

$$\sin^2 \alpha = \frac{4 - 2R}{1 + 2R} \qquad (1)$$

Equation 1 strictly holds only for the case of xy degenerate excitation dipoles. This symmetry requirement is met by porphyrins in general, which have effective D_{4h} symmetry, and we have made this assumption for cytochrome a_3. Although the symmetry of heme a is D_{2h} or lower (Woodruff et al., 1982), with regard to the electronic absorption spectrum in the α-band region the effective symmetry appears to be xy degenerate.

Transients were taken with pump-pulse polarizations parallel and perpendicular to the infrared probe beam as a function of pump power. The percent photodissociation was calculated from a linear fit of the pump power dependence of the anisotropy by ratioing the unpolarized value, ΔA =

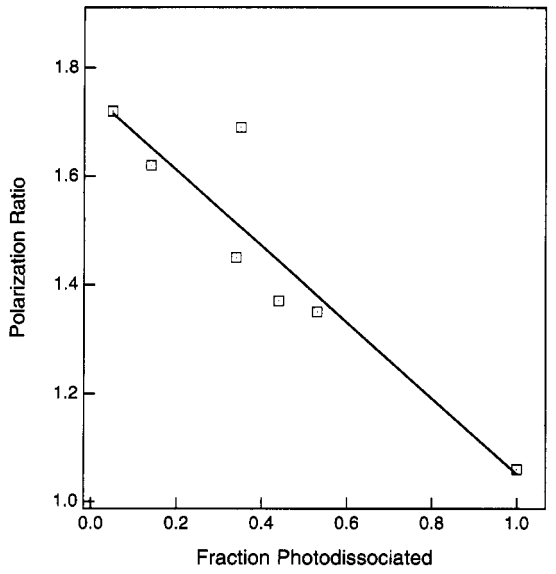

FIGURE 4: Dependence of the picosecond infrared absorption anisotropy (R) of $Fe_{a3}CO$ (1963 cm^{-1}) on percent photodissociation of CO.

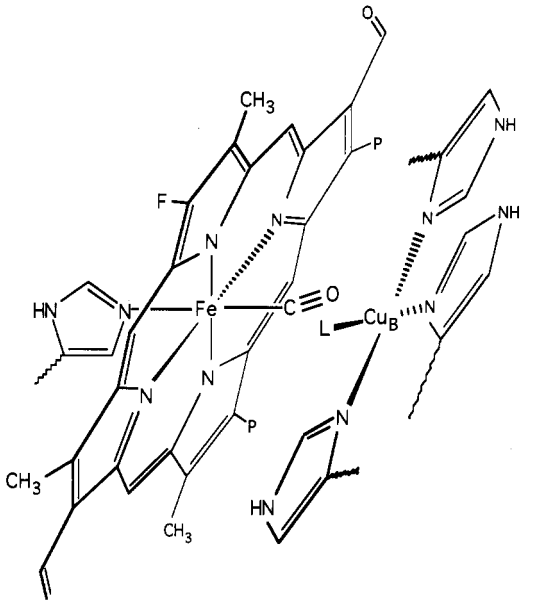

FIGURE 5: Model of the binuclear center showing possible ligands to Cu_B and its position relative to the heme.

$1/2(\Delta A_{\parallel} + \Delta A_{\perp})$, at a given power to its maximum, asymptotic value at high powers. The polarization ratio, R, for $Fe_{a3}CO$, probed at 1963 cm^{-1}, is plotted as a function of percent photodissociation in Figure 4. The value of 1.75 ± 0.06 at 0% photodissociation yields an average angle of 20 ± 3°. When Cu_BCO is probed at 2062 cm^{-1}, a polarization ratio of 1.00 ± 0.05 was observed at all powers. This corresponds to either an average angle of 55 ± 3° or an isotropic orientation (vide infra).

DISCUSSION

The most striking result of this study is the rapidity with which CO transfers from iron to copper, yielding the fully developed, ground state Cu_BCO complex within 1 ps. This suggests that there are no activation barriers to the migration of CO to Cu_B. It is clear that the binuclear Fe_{a3}–Cu_B site is elegantly designed to facilitate rapid transfer of small molecules between the two metals. Furthermore, the observation of a stationary spectrum at 1 ps suggests that the Cu_BCO is vibrationally cool on this time scale, which requires extremely rapid energy transfer out of the newly formed Cu_B–C bond. By considering the structure of the binuclear center together with time scales for bond breakage and formation, energy relaxation and ligand reorganization, and what we know to be the upper limit for the CO transfer time, it is possible to draw conclusions regarding various reaction scenarios.

We first consider the structure of the binuclear center and its CO complexes. As noted previously, the histidine ligands to the binuclear center have been identified by spectroscopic methods and site-directed mutagenesis. Spectroscopic and EXAFS data place the Cu_B within 5 Å of the Fe of cytochrome a_3 (Boelens et al., 1984; Powers & Chance, 1985; Thomson et al., 1985). A model of the binuclear center derived from these data, which illustrates the ligands to each metal and the Fe–Cu distance, is shown in Figure 5.

Specific structural information for the CO complexes of Fe_{a3} and Cu_B is obtained from the linear dichroism data. For CO bound to Fe_{a3}, the angle of 20° measured in this study for the CO vibrational dipole relative to the heme plane normal is in agreement with the 21 ± 2° obtained previously (Dyer et al., 1989b) with 532-nm excitation on the nanosecond time scale [this close agreement validates our procedure for removing the rotational ($\tau_{rotation} \sim 6$ μs) depolarization from the nanosecond data by extrapolation of the polarization ratio to zero time]. The derived angle is strictly the angle between the heme normal and the CO bond axis; separation into bend and tilt angles for the CO–cytochrome a_3 complex is not possible based on this approach. While CO typically binds perpendicularly to the heme plane in protoheme and other heme model compounds (Peng & Ibers, 1976; Scheidt et al., 1981), in proteins steric constraints imposed by the protein structure often lead to bent or tilted configurations. For example, the CO orientation in cytochrome a_3 is similar to that measured by both X-ray scattering (Kuriyan et al., 1986) and picosecond infrared linear dichroism for hemoglobin–CO (18°) and one of the myoglobin–CO conformers (20° and 35°) (Hansen et al., 1989; Moore et al., 1988).

For CO bound to Cu_B, the polarization ratio of 1.0 obtained at 2062 cm^{-1} also agrees with that obtained previously on the nanosecond time scale (Dyer et al., 1989b). A polarization ratio of 1.0 formally corresponds to either of two situations: (1) where the angle relative to the normal of the excitation dipole plane is 54.7° which is coincidentally equal to the "magic angle", or (2) where an isotropic distribution of CO dipoles relative to the pump polarization is present. An isotropic distribution may result from protein reorientation on the experimental time scale or from a truly isotropic distribution of Cu_B–CO sites relative to the heme plane. The rotation time for CcO, measured in previous nanosecond TRIR linear dichroism experiments is about 6 μs and thus cannot contribute significantly to depolarization on the picosecond time scale. Furthermore, the narrow bandwidth for the CO vibration at 2062 cm^{-1} suggests that the CO is in a single, constrained conformation, making it improbable that the Cu_B–CO orientation is isotropic with respect to the heme plane. The weight of evidence is consistent with an orientation of the CO dipole on CuB at an angle near 55° relative to the normal to the heme plane of cytochrome a_3.

It is not known where Cu_B lies relative to Fe_{a3}; consideration of steric effects between the porphyrin and the ligands of Cu_B, however, constrain it to lie on the distal side near the line which is perpendicular to the heme plane and passes through the iron, as illustrated in Figure 5. This suggests that CO may need to move less than 1 Å to be in position to bind to

the copper. However, this requires CO to point toward the heme plane (at a 55° angle from the heme normal), which would result in substantial van der Waals overlap with the porphyrin. These steric constraints probably favor a conformation in which the CO is pointed away from the heme plane. In the latter configuration, the CO must move approximately 4 Å to reach its equilibrium orientation on Cu_B.

Turning to the dynamics, we first consider the bond breakage and formation steps. Femtosecond visible absorption measurements (Stoutland et al., 1991) indicate that the Fe–C bond in CO ligated cytochrome oxidase is completely ruptured within 100 fs after photoexcitation of the heme, possibly on the time scale of the Fe–C vibrational period (520 cm^{-1}, 64 fs). This time scale is consistent with the direct observation of photoinitiated bond *breakage* in small molecules in the gaseous phase (Rosker et al., 1988). The time scale of bond *formation* is less well known, as the rate-limiting step is typically the collision frequency, determined either by gas kinetics or diffusion control. If "free" CO is produced by photodissociation, the rate of bond formation will likely be determined by the rate of diffusion through the protein. Collisions with solvent in CcO are unlikely; evidence from static FTIR studies suggests that the binuclear center is held in a relatively rigid protein environment from which solvent is excluded (Einarsdóttir et al., 1988). FTIR spectra of CO bound to either the Fe_{a3} or Cu_B center show very narrow CO line widths; these bands undergo significant shifts upon deuteriation of the protein, unless the deuteriation is attempted after the reduced CO complex is already formed. The isolation from deuterium effects in the latter case indicates that the binuclear center is closed to solvent in the reduced CO form of the enzyme. However, the protein itself provides the means for collisional energy loss and the possibility of a diffusive-like reaction pathway. In the absence of diffusion, the process of bond formation will be determined by the transit time of CO between metal centers, the energy transfer out of the incipient bond, and any concomitant reorganization processes.

Hochstrasser and co-workers have made estimates for the excess energy, thermalization time, and mean free path for a photodissociated CO molecule in the hemoglobin pocket (Anfinrud et al., 1989). We expect the energetics of dissociation to be similar in hemoglobin and cytochrome oxidase. They estimated that CO can leave the heme with a maximum velocity of 13.6 Å per picosecond. The actual velocity will depend on how the approximately 26 kcal of excess energy above the Fe–C bond dissociation energy is partitioned between the heme and CO. Crystallographic data for hemoglobin show that a CO molecule could travel only about 1 Å before contacting the protein (Kuriyan et al., 1986). If all of the excess energy (the difference between the excitation energy and the Fe–C bond dissociation energy) results in CO translational motion, there is sufficient energy to move by a diffusive mechanism up to 3 Å in 1 ps, assuming no collisional cooling. Since the CO is likely to experience numerous collisions with the protein, however, its motion would be rapidly thermalized, in which case the CO would move in a purely diffusive manner, at ambient temperature, only 1 Å in a picosecond. Accordingly, the observed rate of CO transfer appears to be inconsistent with the formation of free CO and random diffusion to Cu_B.

The close proximity of CO to Cu_B while attached to Fe_{a3} (possibly within van der Waals contact) and the observation that the Cu_BCO complex is fully formed, in its ground state, within 1 ps suggest another possibility. Specifically, "free" CO is never formed, but instead as the Fe–C bond starts to lengthen, CO immediately feels the influence of the Cu_B potential. In this view, the formation of the Cu_B–C bond would be rapid and concurrent with the Fe–C bond rupture. Other studies have shown, however, that CO bound to the heme does not form a bridge to Cu_B in any real bonding sense (Einarsdóttir et al., 1988), meaning that this is a true bond-breakage/formation process.

Regardless of how CO is transferred to the copper site, ligand reorganization and dissipation of bond formation energy occur within 1 ps as the spectrum of the fully formed, ground state complex is seen within this time period. At a minimum, this requires that energy transfer out of the incipient bond (i.e., the Cu_B–C bond) be extremely rapid. The sparse experimental evidence available for inorganic complexes suggests the IVR rates may be relatively slow (i.e., >1 ps) due to the large frequency mismatches present (Heilweil et al., 1988; Rogers et al., 1982, 1983). This is certainly *not* the case here as energy transfer out of the Cu_B–C bond, and any concomitant reorganization processes are complete within a picosecond, which suggests that the protein linkages may be very efficient in transferring energy.

Geminate recombination of the CO was not observed on any time scale; the $Fe_{a3}CO$ IR bleach remains constant from the earliest times investigated (<1 ps) until the CO begins to recombine on the millisecond time scale. Geminate recombination of CO with hemes in proteins or in solution is typically "slow" (nanoseconds) compared to other π-acid ligands such as NO and O_2. This relatively slow rate has been attributed to an electronic (spin) barrier (Petrich et al., 1988) or to a frictional force barrier due to iron displacement opposing rebinding (Chance et al., 1990; Cornelius et al., 1983), which are formed on the time scale of the CO photodissociation and heme spin-state change (100 fs). In CcO, however, a barrier to recombination which lives for microseconds is also formed, namely, the kinetic trapping of CO by Cu_B. This kinetic barrier results from a rate of transfer to Cu_B which is much faster than the intrinsic heme–CO recombination rate. Another consequence of the rapid rate is *quantitative* transfer of CO under kinetic control because binding to Cu_B is so much faster than geminate recombination or escape from the heme pocket.

Longer time scale infrared and UV–vis experiments have shown that CO dissociates from Cu_B on a microsecond time scale ($k_{-1} = 5 \times 10^5\ s^{-1}$), a thermal equilibrium between "Cu_B bound" and "free" CO in solution ($K = 87\ M^{-1}$) is established, and the CO does not return to Fe_{a3} for milliseconds ($k_2 = 1030\ s^{-1}$) . On the time scale that CO leaves Cu_B (1.5 μs), there are no intrinsic heme barriers to recombination with Fe_{a3}, since typical geminate recombination rates are nanoseconds. Another barrier must form which prevents CO recombination prior to 1 ms; possible candidates include a local protein conformational change or the binding of an endogenous ligand which blocks the distal ligation site.

Woodruff et al. (1991) have proposed that the long-lived barrier to CO recombination is formed by the binding of an endogenous ligand (designated as L) to the distal coordination site of cytochrome a_3, *when CO is on* Cu_B. Preliminary evidence for this model was obtained from transient UV–vis absorption experiments in which a long-lived α-band absorption change was observed for cytochrome a_3 following CO photodissociation (Woodruff et al., 1991). This transient is clearly not due to CO liganded enzyme but is also red-shifted by 15 nm from the static absorption spectrum of unligated, fully reduced oxidase. The 6-ps rise and the 1-μs decay of this transient closely correspond to the formation and decay of the

Cu_BCO complex. These observations suggest that a structural change at cytochrome a_3 occurs in association with CO binding to and dissociation from Cu_B. The specific nature of this structural change was investigated using time-resolved resonance Raman and time-resolved magnetic circular dichroism, which indicate that the cytochrome a_3 transient formed following CO photodissociation must be five-coordinate, high spin but with an axial ligand other than imidazole (Woodruff et al., 1991). These results were reconciled with a model in which L binds to Fe_{a3} on the distal side of the heme, while the proximal iron–imidazole bond is broken. In addition, the evidence suggests that L is initially on Cu_B prior to photodissociation of CO and that the transfer of CO to Cu_B triggers the transfer of L to Fe_{a3}.

The picosecond infrared studies presented here provide additional insight into the dynamics of the shuttling of L between metal centers. If the loss of L from Cu_B occurs in 6 ps (the time scale of the cyt a_3 α-band transient), this process should be detectable via changes in the infrared spectrum and linear dichroism of Cu_BCO. Since these infrared observables are unchanged from 1 ps until CO dissociates from Cu_B, no change in ligation at Cu_B likely occurs on this time scale. We conclude that loss of L from Cu_B is rapid and concurrent with the arrival of CO. The binding of L to Fe_{a3} then occurs in a separate, slower (6 ps) step. These results also suggest an approach for substantiating the endogenous ligand "L" model. Since we have identified transients in the pathway of CO out of the protein for which L is bound to different metal centers, it should be possible to identify a vibrational mode in TRIR difference spectra associated with L in these different states.

CONCLUSIONS

Picosecond time-resolved visible pump/infrared probe experiments have been used to study the photoinitiated transfer of CO from Fe_{a3} to Cu_B in fully reduced, carbonmonoxy cytochrome *c* oxidase. Complete transfer of photodissociated CO with full formation of the Cu_BCO complex in the ground state occurs within 1 ps. This remarkably fast transfer provides insight into possible mechanisms for the transfer of small molecules between the two metals. In addition, induced linear dichroism measurements show that the CO is oriented at an angle of 20° to the heme normal when bound to cytochrome a_3, similar to carbonmonoxy hemoglobin and one of the carbonmonoxy-myoglobin conformers. The CO dipole was found to be oriented near 55° off the heme normal when bound to Cu_B.

An important question is the relevance of these results to the function of the enzyme. Is binding to Cu_B an obligatory step in the movement of small molecules (oxygen in particular) in and out of the reactive center, or are these results peculiar to CO photodissociation? Similar studies with different exogenous ligands such as NO, RCN, and CN^-, and also with different oxidation states of the metals, are in progress and should provide further insight into ligation dynamics and kinetics which are important to the function of the enzyme.

Finally, we note the significance of these results in elucidating fundamental phenomena in the dynamics of bond formation in general and the coordination of ligands in particular. Our study implies that cytochrome oxidase may function as a unique system for addressing these issues, in the same sense that the photosynthetic reaction center has become a paradigm for fundamental issues in electron transfer dynamics. Few systems offer a comparable opportunity to observe bond formation directly in the absence of control by diffusion or gas kinetics. We are aware of no other systems where the ability to directly observe bond formation dynamics approaches the dephasing time of the vibrational transition associated with bonding [for $\nu(Cu_BCO)$, $\Delta\nu = 8$ cm^{-1}, which puts an upper limit on the dephasing time of 600 fs]. We are continuing our studies with emphasis on these questions.

REFERENCES

Alben, J. O., Moh, P. P., Fiamingo, F. G., & Altschuld, R. A. (1981) *Proc. Natl. Acad. Sci. U.S.A. 78,* 234–237.

Anfinrud, P. A., Han, C., & Hochstrasser, R. M. (1989) *Proc. Natl. Acad. Sci. U.S.A. 86,* 8387–8391.

Blackmore, R. S., Greenwood, C., & Gibson, Q. H. (1991) *J. Biol. Chem. 266,* 19245–19249.

Boelens, R., Rademaker, H., Wever, R., & Gelder, B. F. V. (1984) *Biochim. Biophys. Acta 765,* 196–209.

Breton, J., Martin, J. L., Fleming, G. R., & Lambry, J. C. (1988) *Biochemistry 27,* 8276–8284.

Chance, M. R., Courtney, S. H., Chavez, M. D., Ondrias, M. R., & Friedman, J. M. (1990) *Biochemistry 29,* 5537–5545.

Cornelius, P. A., Hochstrasser, R. M., & Steele, A. W. (1983) *J. Mol. Biol. 163,* 119–128.

Dyer, R. B., Einarsdóttir, Ó., Killough, P. M., López-Garriga, J. J., & Woodruff, W. H. (1989a) *J. Am. Chem. Soc. 111,* 7657–7659.

Dyer, R. B., López-Garriga, J. J., Einarsdóttir, Ó., & Woodruff, W. H. (1989b) *J. Am. Chem. Soc. 111,* 8962–8963.

Dyer, R. B., Peterson, K. A., Stoutland, P. O., & Woodruff, W. H. (1991) *J. Am. Chem. Soc. 113,* 6276–6277.

Einarsdóttir, Ó., Choc, M. G., Weldon, S., & Caughey, W. S. (1988) *J. Biol. Chem. 263,* 13641–13654.

Einarsdóttir, Ó., Killough, P. M., Fee, J. A., & Woodruff, W. H. (1989) *J. Biol. Chem. 264,* 2405–2408.

Einarsdóttir, Ó., Dyer, R. B., Lemon, D. D., Killough, P. M., Hubig, S. M., Atherton, S. J., López-Garriga, J. J., Palmer, G., & Woodruff, W. H. (1993) *Biochemistry 32,* 12013–12024.

Fiamingo, F. G., Altschuld, R. A., Moh, P. P., & Alben, J. O. (1982) *J. Biol. Chem. 257,* 1639–1650.

Gibson, Q. H., & Greenwood, C. (1963) *Biochem. J. 86,* 541–554.

Greenwood, C., & Gibson, Q. H. (1967) *J. Biol. Chem. 242,* 1782–1787.

Hansen, P. A., Moore, J. N., & Hochstrasser, R. M. (1989) *Chem. Phys. 131,* 49–62.

Heilweil, E. J., Cavanagh, R. R., & Stephenson, J. C. (1987) *Chem. Phys. Lett. 134,* 181.

Heilweil, E. J., Cavanagh, R. R., & Stephenson, J. C. (1988) *J. Chem. Phys. 89,* 230–239.

Kuriyan, J., Wilz, S., Karplus, M., & Petsko, G. A. (1986) *J. Mol. Biol. 192,* 133–154.

Moore, J. N., Hansen, P. A., & Hochstrasser, R. M. (1988) *Proc. Natl. Acad. Sci. U.S.A. 85,* 5062–5066.

Ormos, P., Braunstein, D., Frauenfelder, H., Hong, M. K., Lin, S.-L., Sauke, T. B., & Young, R. D. (1988) *Proc. Natl. Acad. Sci. U.S.A. 85,* 8492–8496.

Peng, S.-M., & Ibers, J. A. (1976) *J. Am. Chem. Soc. 98,* 8032–8036.

Petrich, J. W., & Martin, J. L. (1989) *Chem. Phys. 131,* 31–47.

Petrich, J. W., Poyart, C., & Martin, J. L. (1988) *Biochemistry 27,* 4049–4060.

Powers, L., & Chance, B. (1985) *J. Inorg. Biochem. 23,* 207–217.

Rogers, P., Montague, D. C., Frank, J. P., Tyler, S. C., & Rowland, F. S. (1982) *Chem. Phys. Lett. 89,* 9.

Rogers, P. J., Selco, J. I., & Rowland, F. S. (1983) *Chem. Phys. Lett. 97,* 313.

Rosker, M. J., Dantus, M., & Zewail, A. H. (1988) *J. Chem. Phys. 89,* 6113–6128.

Scheidt, W. R., Haller, K. J., Fons, M., Mashiko, T., & Reed, C. A. (1981) *Biochemistry 20,* 3653–3657.

Schoenlein, R. W., Peteanu, L. A., Mathies, R. A., & Shank, C. V. (1991) *Science 254,* 412–415.

Shapleigh, J. P., Hosler, J. P., Tecklenburg, M. M. J., Kim, Y., Babcock, G. T., Gennis, R. B., & Ferguson-Miller, S. (1992) *Proc. Natl. Acad. Sci. U.S.A. 89,* 4786–4790.

Stoutland, P. O., Lambry, J.-C., Martin, J.-L., & Woodruff, W. H. (1991) *J. Phys. Chem. 95,* 6406–6408.

Stoutland, P. O., Dyer, R. B., & Woodruff, W. H. (1992) *Science 257,* 1913–1917.

Surerus, K. K., Oertling, W. A., Fan, C., Gurbiel, R. J., Einarsdóttir, Ó., Antholine, W. E., Dyer, R. B., Hoffman, B. M., Woodruff, W. H., & Fee, J. A. (1992) *Proc. Natl. Acad. Sci. U.S.A. 89,* 3195–3199.

Thomson, A. J., Greenwood, C., Gadsby, P. M. A., Peterson, J., Eglinton, D. G., Hill, B. C., & Nicholls, P. (1985) *J. Inorg. Biochem. 23,* 187–197.

Varotsis, C., Woodruff, W. H., & Babcock, G. T. (1989) *J. Am. Chem. Soc. 111,* 6439–6440.

Wikström, M., Krab, K., & Saraste, M. (1981) *Cytochrome Oxidase, A Synthesis.* Academic Press, New York.

Woodruff, W. H., Kessler, R. J., Ferris, N. S., Dallinger, R. F., Carter, K. R., Antalis, T. M., & Palmer, G. (1982) *Adv. Chem. Ser. 201,* 625–659.

Woodruff, W. H., Einarsdóttir, Ó., Dyer, R. B., Bagley, K. A., Palmer, G., Atherton, S. J., Goldbeck, R. A., Dawes, T. D., & Kliger, D. S. (1991) *Proc. Natl. Acad. Sci. U.S.A. 88,* 2588–2592.

Woodruff, W. H., Dyer, R. B., & Einarsdóttir, Ó. (1993) in *Biomolecular Spectroscopy Part B* (Clark, R. J. H., & Hester, R. E., Eds.) pp 189–233, John Wiley & Sons Ltd., Chichester.

Yen, R., Shank, C. V., & Hirlimann, C. (1983) *Mater. Res. Soc. Symp. Proc. 13,* 13–16.

Yoshikawa, S., Choc, M. G., O'Toole, M. C., & Caughey, W. S. (1977) *J. Biol. Chem. 252,* 5498–5508.